

A. Görgen,^{1,2} R.M. Clark,¹ M. Cromaz,¹ P. Fallon,¹ G.B. Hagemann,³ H. Hübel,⁴ I.Y. Lee,¹ A.O. Macchiavelli,¹
G. Sletten,³ D. Ward,¹ and R. Bengtsson⁵

¹*Nuclear Science Division, Lawrence Berkeley National Laboratory, Berkeley, California 94720*

²*DAPNIA/SPhN, CEA Saclay, F-91191 Gif-sur-Yvette, France*

³*The Niels Bohr Institute, Blegdamsvej 17, DK-2100 Copenhagen Ø, Denmark*

⁴*HISKP, Universität Bonn, Nussallee 14-16, D-53115 Bonn, Germany*

⁵*Department of Mathematical Physics, Lund Institute of Technology, S-22362 Lund, Sweden*

(February 25, 2004)

Lifetimes of states in the triaxial strongly deformed bands of ^{163}Lu have been measured with the Gammasphere spectrometer using the Doppler-shift attenuation method. The bands have been interpreted as wobbling-phonon excitations from the characteristic electromagnetic properties of the transitions connecting the bands. Quadrupole moments are extracted for the zero-phonon yrast band and, for the first time, for the one-phonon wobbling band. The very similar results found for the two bands suggest a similar intrinsic structure and support the wobbling interpretation. While the in-band quadrupole moments for the bands show a decreasing trend towards higher spin, the ratio of the interband to the in-band transition strengths remains constant. Both features can be understood by a small increase in triaxiality towards higher spin. Such a change in triaxiality is also found in cranking calculations, to which the experimental results are compared.

PACS numbers: 21.10.Tg; 21.60.Ev; 23.20.Lv; 27.70.+q

Triaxiality in nuclei and related phenomena have long been predicted but are difficult to prove experimentally. A region of stable triaxiality is predicted in the neutron-deficient Lu and Hf isotopes around $N = 94$, where cranking calculations give local triaxial minima at large deformation (triaxial strongly deformed, TSD) with $(\epsilon_2, \gamma) \approx (0.4, \pm 20^\circ)$ in the total energy surfaces. These nuclei have been studied extensively and many rotational structures that can be associated with TSD minima have been observed in several nuclides. The first proof of stable triaxiality was not the observation of these bands as such, but rather from the fact that some of the bands in odd-mass Lu isotopes can be described as wobbling-phonon excitations [1–4].

The wobbling motion is an excitation mode unique to a triaxial body. While the nucleus favors the rotation about the axis with the largest moment of inertia, it can transfer a quantized amount of angular momentum to the other axes, resulting in a sequence of rotational bands built on the same intrinsic structure. In the high-spin limit the energies of the wobbling bands can be separated into rotation about the principal axis and the wobbling motion [5]: $E_R(I, n_w) = I(I+1)/(2\mathcal{I}_x) + \hbar\omega_w(n_w + 1/2)$, where n_w is the wobbling phonon number and ω_w is the wobbling frequency which depends only on the three moments of inertia with respect to the three principal axes. A characteristic fingerprint of the wobbling mode is the occurrence of $E2$ interband transitions with $\Delta I = 1$ from bands with n_w wobbling phonons to bands with $n_w - 1$ which compete with the very enhanced $E2$ transitions within the strongly deformed bands. The strength of the collective interband transitions $B(E2; n_w \rightarrow n_w - 1)$ is expected to be proportional to n_w/I . The presence of a particle with its spin aligned to the rotation axis, an

$i_{13/2}$ proton in the case of the TSD bands in odd-mass Lu isotopes, adds an additional degree of freedom to the wobbling motion, and its presence may stabilize the triaxial core. The influence of the aligned proton has been studied in particle-rotor calculations [6,7].

The wobbling mode was first reported in ^{163}Lu [1,2], where three TSD bands were identified as the zero-, one-, and two-phonon bands. The evidence was based on the characteristic properties of the interband transitions, for which the $E2$ strength of the $\Delta I = 1$ transitions was shown to exhibit the expected pattern. Shortly afterwards, similar evidence for the wobbling mode was found in ^{165}Lu [3], ^{167}Lu [4], and possibly also in ^{161}Lu [8].

It is interesting to note that cranking calculations predict the Hf isotopes around ^{166}Hf to be even better candidates for TSD bands [9]. Experimental evidence for such bands, however, exists only in ^{168}Hf [10], ^{170}Hf [11], and in ^{174}Hf [12]. There is a discrepancy between the theoretical prediction of the region of TSD bands and where they are experimentally found. More experimental information is needed to determine the exact position of the intruder subshells which lead to the occurrence of triaxial minima.

Lifetime measurements in the excited TSD bands provide a crucial test for the wobbling interpretation. Very similar $B(E2)$ strengths for the in-band transitions are expected, as the wobbling bands are built on the same intrinsic structure. Measurements have been attempted in ^{163}Lu [13–15], but only for the yrast band and the different experiments are not in agreement.

In this paper we present data on a precision lifetime measurement in ^{163}Lu , which provides the first measurement for the proposed one-phonon wobbling band (TSD2) and resolves the discrepancy in previous data on

TSD1. These new data will be used to gain important insight into the evolution of triaxiality as a function of spin that can simultaneously explain the observed spin dependence of the in-band and interband $B(E2)$ values.

In the experiment, high-spin states in ^{163}Lu were populated in the reaction $^{123}\text{Sb}(^{44}\text{Ca},4n)$ at a beam energy of 190 MeV. The beam was accelerated by the 88-Inch Cyclotron of the Lawrence Berkeley National Laboratory. The target comprised a 1 mg/cm^2 foil of ^{123}Sb enriched to 99.3% on a gold backing of 12 mg/cm^2 to slow down and finally stop the recoils. Gamma rays were detected with the Gammasphere array [16], which for this experiment consisted of 102 large-volume Compton-suppressed germanium detectors grouped into 17 rings that cover angles from 17.3° to 162.7° with respect to the beam direction. A total of 1.6×10^9 events in which at least five germanium detectors gave coincident signals were recorded in three days and stored in an indexed, energy-ordered database using the BLUE software [17]. Spectra for each angle were sorted from the database under various gating conditions.

The level lifetimes were extracted by the analysis of the Doppler-broadened line shapes observed at various angles with respect to the beam direction. The program of Wells and Johnson [18], based on the program of Baccalar [19], was used for this analysis. The stopping of the recoils was simulated using Monte Carlo methods with 5000 histories and a time step of 0.001 ps following the prescription of Gascon et al. [20]. For the electronic stopping power the tables of Northcliffe and Schilling [21] were used with a shell correction. Line shapes were fitted simultaneously for multiple transitions and different combinations of angles. The side feeding was modeled by a cascade of five transitions with the same moment of inertia as the in-band transitions. The intensity of the side feeding was constrained to the experimentally observed value. It was difficult to determine the side-feeding intensity for the states in the upper part of the bands where the line shapes are very broad. In these cases the intensities were taken from an earlier thin-target experiment [22]. This is justified since the intensities for the transitions lower in the bands agree well. The quadrupole moment for transitions feeding into the bands was allowed to vary only within 15% of that of the in-band transitions for initial fits of single states and it was fixed to this initial value for the subsequent fits of the entire cascade. The side-feeding quadrupole moment was generally found to be a few percent smaller than the in-band quadrupole moment, in agreement with the earlier measurement by Schönwaßer et al. [14]. Furthermore, for some transitions in band TSD1 it was possible to gate from above, eliminating the effects of side feeding. The results obtained from gating above and gating below were in good agreement. The influence of the direct feeding from TSD2 into TSD1 was neglected since this accounts only for about 5% of the total feeding and the lifetimes

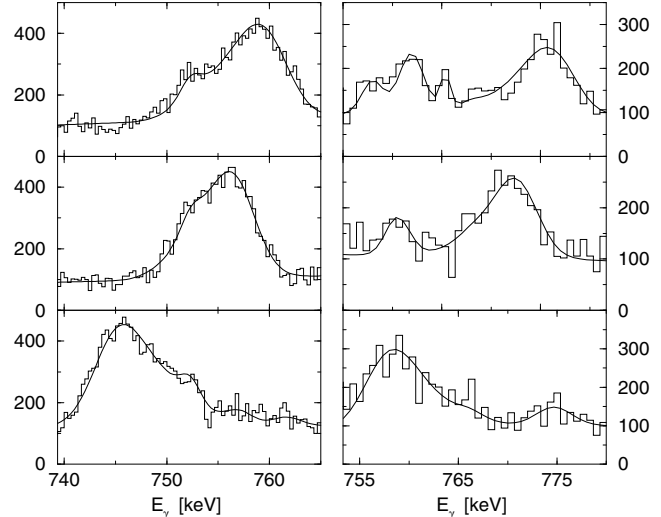


FIG. 1. Spectra and fitted line shapes for the 753 keV transition of band TSD1 (left) and for the 766 keV transition of band TSD2 (right) observed at 50° (top), 70° (center), and 130° (bottom). Contaminant peaks are present and included in the fit.

in band TSD2 are very similar to those in TSD1, as will be shown. Other fit parameters include a linear background and the intensities of contaminant peaks. These parameters were also determined in an initial fit to the individual transitions and then fixed for subsequent fits to multiple transitions. The errors were derived from the covariance matrix of the χ^2 minimization and from the spread of the results obtained for different combinations of angles. Systematic errors originating from the choice of stopping powers are not included. Examples of typical line shape fits for transitions in bands TSD1 and TSD2 are shown in Fig. 1.

Eight lifetimes of states in TSD1 and seven in TSD2 were determined from the Doppler-broadened line shapes. The results are summarized in Table I. The values for TSD1 agree within errors with the earlier measurement of Schönwaßer et al. [14], in which the transition quadrupole moments of the 753, 806, and 858 keV transitions were found to be $8.1^{+1.0}_{-1.1}$, $8.3^{+1.9}_{-1.1}$, and $8.0^{+1.6}_{-1.5}$ b, respectively. They are, however, in disagreement with the much larger values reported by Schmitz et al. [13]. Due to the far higher efficiency of the Gammasphere spectrometer compared to the GaSp and Nordball spectrometers, with which the earlier data were taken, the new data have smaller uncertainties. In the present data there are about 15 times more counts in the peaks (for each angle) compared to the GaSp data [14], and about 35 times more than in the Nordball data [13]. In addition, data at more angles were recorded in the present experiment. We now feel that the weight of evidence is against the results reported by Schmitz et al. [13].

While the measured lifetimes in band TSD1 can be directly converted into the $B(E2)$ strengths, the ones mea-

TABLE I. Lifetimes, $B(E2)$ values, and transition quadrupole moments Q_t for the in-band transitions in bands TSD1 (upper part) and TSD2 (lower part).

I_i^π	E_γ [keV]	τ [ps]	$B(E2)$ [e^2b^2]	Q_t [b]
41/2 ⁺	578.6	0.364 ^{+0.073} _{-0.085}	3.45 ^{+0.80} _{-0.69}	9.93 ^{+1.14} _{-0.99}
45/2 ⁺	639.0	0.250 ^{+0.035} _{-0.039}	3.07 ^{+0.48} _{-0.43}	9.34 ^{+0.72} _{-0.65}
49/2 ⁺	697.0	0.202 ^{+0.021} _{-0.023}	2.45 ^{+0.28} _{-0.25}	8.32 ^{+0.47} _{-0.42}
53/2 ⁺	752.6	0.119 ^{+0.009} _{-0.010}	2.84 ^{+0.24} _{-0.22}	8.93 ^{+0.38} _{-0.35}
57/2 ⁺	805.6	0.096 ^{+0.011} _{-0.012}	2.50 ^{+0.32} _{-0.29}	8.37 ^{+0.54} _{-0.49}
61/2 ⁺	857.7	0.088 ^{+0.010} _{-0.011}	1.99 ^{+0.26} _{-0.23}	7.45 ^{+0.49} _{-0.43}
65/2 ⁺	909.7	0.067 ^{+0.010} _{-0.015}	1.95 ^{+0.44} _{-0.30}	7.37 ^{+0.82} _{-0.57}
69/2 ⁺	962.5	0.047 ^{+0.017} _{-0.011}	2.10 ^{+0.80} _{-0.48}	7.63 ^{+1.46} _{-0.88}
47/2 ⁺	654.6	0.215 ^{+0.037} _{-0.048}	2.56 ^{+0.57} _{-0.44}	8.51 ^{+0.95} _{-0.73}
51/2 ⁺	711.2	0.144 ^{+0.017} _{-0.022}	2.67 ^{+0.41} _{-0.33}	8.67 ^{+0.66} _{-0.53}
55/2 ⁺	766.2	0.095 ^{+0.013} _{-0.018}	2.81 ^{+0.53} _{-0.41}	8.88 ^{+0.83} _{-0.64}
59/2 ⁺	819.9	0.087 ^{+0.026} _{-0.037}	2.19 ^{+0.94} _{-0.65}	7.82 ^{+1.66} _{-1.15}
63/2 ⁺	872.9	0.064 ^{+0.013} _{-0.021}	2.25 ^{+0.75} _{-0.48}	7.91 ^{+1.32} _{-0.84}
67/2 ⁺	926.5	0.075 ^{+0.017} _{-0.025}	1.60 ^{+0.52} _{-0.37}	6.66 ^{+1.09} _{-0.76}
71/2 ⁺	980.2	0.056 ^{+0.017} _{-0.029}	1.61 ^{+0.82} _{-0.49}	6.68 ^{+1.70} _{-1.02}

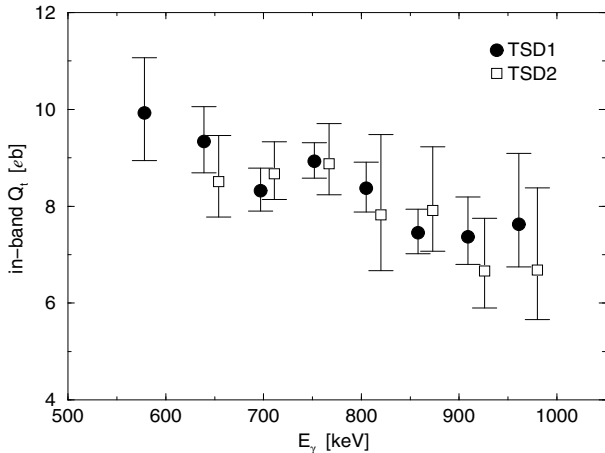


FIG. 2. Transition quadrupole moments of the in-band transitions in bands TSD1 and TSD2.

sured in TSD2 have to be corrected for the competing decay out of the band in order to get the strength of the in-band transitions. Since it is difficult to obtain the branching ratios from the Doppler-broadened peaks in the present experiment, the values obtained in the thin-target experiment [22] were used to correct for the decay out.

For a triaxial nucleus, K is not a good quantum number and in order to extract the quadrupole moments from the $B(E2)$ values, one has to use a distribution of different K values: $B(E2) = \frac{5}{16\pi}(eQ)^2 \sum_K c_K^2 \langle I_i K 20 | I_f K \rangle^2$. Cranking calculations with the *Ultimate Cranker* code [23] show that the wave function has a pure $i_{13/2}$ configuration aligned with the rotational axis. Assuming such a pure configuration, the coefficients c_K can be calculated using Wigner's D -functions, $D_{jK}^j(0, \frac{\pi}{2}, 0)$ with $j = 13/2$. The resulting in-band quadrupole moments are summarized in Table I and plotted in Fig. 2.

The values for the two bands show a striking similar-

ity. This is expected in the wobbling-phonon picture, as the bands are built on the same intrinsic structure. One would expect a difference of only about 4% in the quadrupole moments due to the tilting of the core angular momentum for the one-phonon wobbling band and therefore slightly different vector coupling coefficients. The identity of the quadrupole moments cannot stand as a proof alone, but is a necessary condition to be fulfilled by wobbling bands and is, therefore, further evidence for the wobbling motion and stable triaxiality.

Both bands exhibit a decrease in the $B(E2)$ and Q_t values as the spin increases. The fact that both bands have not only very similar values, but also show the same change of these values further strengthens the argument that the bands are built on the same structure. The experimental values may be compared to the *Ultimate Cranker* calculations, where the quadrupole moments are calculated directly from the wave functions. This comparison is shown in the upper part of Fig. 3 and allows us to associate the band with the second minimum at $(\epsilon_2, \gamma) \approx (0.4, +20^\circ)$. The calculated quadrupole moment for the normal deformed minimum at $(\epsilon_2, \gamma) \approx (0.2, 0^\circ)$ is shown for comparison. The calculations reproduce a small decrease in the quadrupole moment due to an increase in the triaxiality parameter γ from $\sim 19.5^\circ$ to 21.5° and a slight decrease in quadrupole deformation ϵ_2 from ~ 0.40 to 0.38 over the relevant spin region. The deformation parameters are displayed in the lower part of Fig. 3. However, the decrease in the calculations is not as pronounced as in the experimental data.

The new lifetime results for band TSD2 allow, for the first time, to establish the absolute $B(E2)$ and $B(M1)$ values for the transitions connecting bands TSD2 and TSD1. They are shown in Table II, where an average value of the mixing ratio $\delta = -3.10^{+0.36}_{-0.44}$ was used, taken from a measurement of the angular correlation and linear polarization of the transitions in a previous experiment [1,22]. This average value did not vary significantly up to spin 51/2 and was used to extract the $B(E2)$ and $B(M1)$ values also at higher spin.

Due to the combined uncertainties of the lifetimes, the branching ratios [22], and the mixing ratio [1], the errors are too large to determine the spin dependence of the interband $B(E2)$ strengths, which is one of the key observable signatures of the wobbling motion and expected to be proportional to n_w/I . However, it is possible to use the ratio of the interband to in-band $B(E2)$ values for which the uncertainties of the lifetimes do not enter, and compare them to the particle-rotor calculations [6,7], which can be expected to produce realistic electromagnetic transition moments due to an exact treatment of the angular momentum coupling. This is illustrated in Fig. 4. The $B(E2)$ ratios are constant and do not follow the expected dependence on spin. However, this ratio strongly depends on the triaxiality parameter γ , as $B(E2;out) \propto \sin^2(\gamma + 30^\circ)$ and $B(E2;in) \propto \cos^2(\gamma + 30^\circ)$. Together

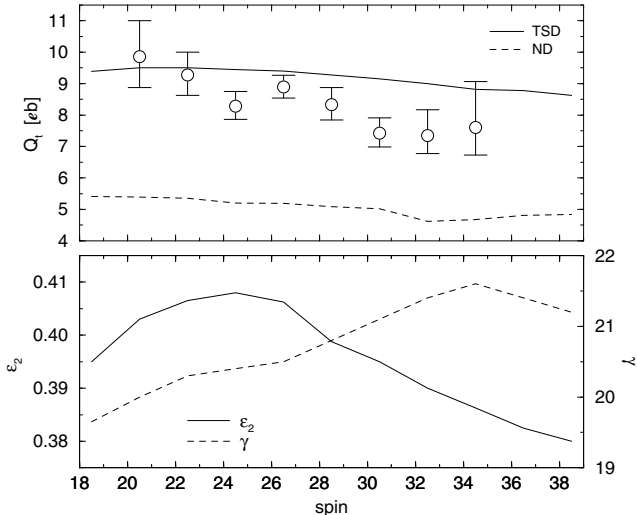


FIG. 3. Comparison of the transition quadrupole moments of band TSD1 with cranking calculations for the TSD and the normal deformed minimum (upper panel). The lower panel shows the quadrupole deformation (solid line) and triaxiality (dashed line) at the minimum in the total energy surface as a function of spin.

TABLE II. $B(E2)$ and $B(M1)$ values for the connecting transitions from TSD2 to TSD1.

I_i^π	E_γ [keV]	$B(E2)$ [e^2b^2]	$B(M1)$ [μ_N^2]
$47/2^+$	658.9	$0.54^{+0.13}_{-0.11}$	$0.017^{+0.006}_{-0.005}$
$51/2^+$	673.2	$0.54^{+0.09}_{-0.08}$	$0.017^{+0.005}_{-0.005}$
$55/2^+$	686.8	$0.70^{+0.18}_{-0.15}$	$0.024^{+0.008}_{-0.007}$
$59/2^+$	701.1	$0.65^{+0.34}_{-0.26}$	$0.023^{+0.013}_{-0.011}$
$63/2^+$	716.3	$0.66^{+0.29}_{-0.24}$	$0.024^{+0.012}_{-0.010}$

with the observed decrease of the transition quadrupole moments of the in-band transitions, this behavior indicates a stronger increase in triaxiality towards higher spin than found in the cranking calculations. An increase from $\gamma \approx 16^\circ$ to $\gamma \approx 22^\circ$ would explain the pronounced decrease in the in-band quadrupole moments and, at the same time, the constant $B(E2)$ ratio for the out-of-band transitions, so that a consistent overall description of the new experimental data is reached.

In summary, lifetimes of states in the TSD bands 1 and 2 in ^{163}Lu were measured using the Doppler-shift attenuation method. The in-band $B(E2)$ values and quadrupole moments for the two bands are very similar and suggest that the bands are built on the same intrinsic structure. Furthermore, the values show a decrease towards higher spin for both bands which is qualitatively reproduced by cranking calculations. The ratio of interband to in-band $B(E2)$ values is found to be constant as a function of spin. We propose that the decrease in the in-band $B(E2)$ and the constant interband $B(E2)$ have the same physical origin and correspond to an increase in the triaxiality with spin, in qualitative agreement with cranking calculations, although slightly

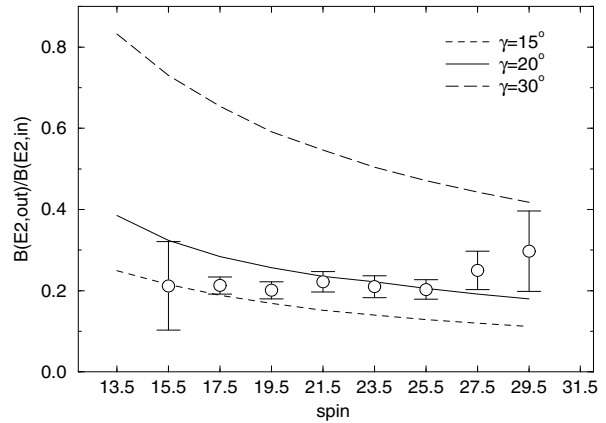


FIG. 4. Ratio of the out-of-band to in-band $B(E2)$ values in comparison with particle-rotor calculations for different values of γ .

stronger than predicted. The new results support the interpretation of the TSD bands as wobbling-phonon excitations and give an experimental handle on the triaxiality parameter γ .

This research was supported in part by the US DoE under contract No. DE-AC03-76SF00098, the Danish Science Foundation, and the German BMBF under contract 06 BN 907. We wish to thank the staff of the 88-Inch Cyclotron at Berkeley, and Ikuko Hamamoto for communicating and discussing theoretical results.

- [1] S.W. Ødegård et al., Phys. Rev. Lett. 86, 5866 (2001)
- [2] D.R. Jensen et al., Phys. Rev. Lett. 89, 142503 (2002)
- [3] G. Schönwaßer et al., Phys. Lett. B552, 9 (2003)
- [4] H. Amro et al., Phys. Lett. B553, 197 (2003)
- [5] A. Bohr and B. Mottelson, *Nuclear Structure*, (Benjamin, New York, 1975), Vol. II, pp. 190 ff.
- [6] I. Hamamoto, Phys. Rev. C 65, 044305 (2002)
- [7] I. Hamamoto, G.B. Hagemann, Phys. Rev. C 67, 014319 (2003)
- [8] P. Bringel et al., to be published
- [9] R. Bengtsson and H. Ryde, to be published
- [10] H. Amro et al., Phys. Lett. B506, 39 (2001)
- [11] A. Neuffer et al., Eur. Phys. J. A 15, 439 (2002)
- [12] M.K. Djongolov et al., Phys. Lett. B560, 24 (2003)
- [13] W. Schmitz et al., Phys. Lett. B303, 230 (1993)
- [14] G. Schönwaßer et al., Eur. Phys. J. A 13, 291 (2002)
- [15] G. Schönwaßer et al., Eur. Phys. J. A 15, 435 (2002)
- [16] I.Y. Lee, Nucl. Phys. A520, 641c (1990)
- [17] M. Cromaz et al., Nucl. Instrum. Methods Phys. Res. A 462, 519 (2001)
- [18] J.C. Wells and N. Johnson, private communication
- [19] J.C. Bacelar et al., Phys. Rev. C 35, 1170 (1987)
- [20] J. Gascon et al., Nucl. Phys. A 513, 344 (1990)
- [21] L.C. Northcliffe and R.F. Schilling, Nucl. Data Tables 7, 233 (1970)
- [22] D.R. Jensen et al., Nucl. Phys. A703, 3 (2002)
- [23] T. Bengtsson, Nucl. Phys. A 512, 124 (1990)